Spin-orbit splittings and energy band gaps calculated with the Heyd-Scuseria-Ernzerhof screened hybrid functional

Juan E. Peralta, Jochen Heyd, and Gustavo E. Scuseria
Department of Chemistry, Rice University, Houston, Texas 77005-1892, USA

Richard L. Martin
Theoretical Division and Seaborg Institute for Transactinium Science, Los Alamos National Laboratory, Los Alamos, New Mexico 87545, USA

(Received 12 May 2006; revised manuscript received 23 June 2006; published 4 August 2006)

We assess the Heyd-Scuseria-Ernzerhof (HSE) screened Coulomb hybrid density functional for the calculation of spin-orbit (SO) splittings and energy band gaps. We have employed a set of 23 semiconductors with available experimental data, including group IV elements, and group III-V, II-VI, and IB-VII compounds. The spin-orbit interaction is included in the calculations using relativistic effective core potentials within a second-variation approximation. HSE errrors are similar to those obtained previously without including SO in the calculation and using a weighted average of the SO split bands for the reference value [J. Chem. Phys. **123**, 174101 (2005)]. Here we explicitly show that the same good agreement remains after explicitly including SO interaction in the calculations and comparing directly to experimental energy band gaps.

DOI: 10.1103/PhysRevB.74.073101 PACS number(s): 71.15.Mb

The performance of density functional theory (DFT) in its local spin density (LSDA) and generalized gradient approximation (GGA) has been extensively analyzed in solid state physics. Improved functionals from the meta-generalized-gradient approximation family [such as the Tao-Perdew-Staroverov-Scuseria[1] (TPSS) functional] have been shown to predict structural properties (for instance, lattice constants and bulk moduli) of better quality than LSDA and GGA,[2–4] while energy band gaps obtained as Kohn-Sham band energy differences with these functionals fail to reproduce experimental gaps.[5,6] Other approaches, such as the "scissor operator,"[7] the LSDA+U,[8] and quasiparticle Green's-function-based methods,[9] like the *GW* approximation,[10] are more prominent for this task.

Hybrid functionals (which include a portion of Hartree-Fock exchange) have been successfully applied in the calculation of thermochemical properties of molecules, in addition to yielding good structural properties.[11] The Heyd-Scuseria-Ernzerhof (HSE) hybrid functional[12,13] originated as an alternative approach that can be efficiently applied to solids. HSE employs screened short-range Hartree-Fock exchange instead of the full exact exchange, drastically reducing the computational requirements and, at the same time, overcoming the known problems of Hartree-Fock exchange.[14] The expression for the HSE exchange-correlation energy is

$$E_{xc}^{\mathrm{HSE}} = aE_x^{\mathrm{HF,SR}} + (1-a)E_x^{\mathrm{PBE,SR}} + E_x^{\mathrm{PBE,LR}} + E_c^{\mathrm{PBE}}, \quad (1)$$

where $E_x^{\mathrm{HF,SR}}$ is the short-range Hartree-Fock exchange, $E_x^{\mathrm{PBE,SR}}$ and $E_x^{\mathrm{PBE,LR}}$ are the short-range and long-range components of the Perdew-Burke-Ernzerhof[15] (PBE) exchange functional, respectively, and $a=1/4$ is the Hartree-Fock exchange mixing parameter (determined via perturbation theory[16,17]). In HSE, the short-range and long-range partition in Eq. (1) is carried out splitting the Coulomb operator as

$$\frac{1}{r} = \underbrace{\frac{\mathrm{erfc}(\omega r)}{r}}_{\mathrm{SR}} + \underbrace{\frac{\mathrm{erf}(\omega r)}{r}}_{\mathrm{LR}}, \quad (2)$$

where erf and erfc are the error and complementary error functions, respectively, and ω is the screening parameter. The functional form of HSE is based on the PBEh hybrid functional (also known in the literature as PBE1PBE and PBE0).[18,19] A detailed derivation of the individual terms of HSE can be found in Refs. 12, 13, and 20. The HSE form can be viewed as an adiabatic connection functional only for the short-range portion of exchange, whereas long-range exchange and correlation are treated at the PBE GGA level.

We have recently shown that HSE gives improved lattice constants and energy band gaps compared to traditional functionals (which do not include Hartree-Fock exchange) using a set of 40 semiconductors (SC/40).[4] We are aware of a recent independent study of the performance of HSE for solids carried out with a plane-waves-based computational program.[21] This study reached similar conclusions to ours for semiconductors, but pointed out some limitations for metals. Here, we extend our previous benchmark[4] by including the spin-orbit (SO) interaction. To this end, we have selected a subset of the SC/40 with available experimental SO splittings and band gaps (two group IV elements, seven group III-V compounds, and seven group II-VI compounds), and we have evaluated these properties using the HSE functional. Furthermore, we have also included six group IB-VII compounds with available experimental values: γ-CuCl, γ-CuBr, γ-CuI, AgCl, AgBr, and γ-AgI. In Ref. 4, we used the weighted average of the experimental SO splitting (whenever available) to obtain the reference band gap to compare with our scalar relativistic (i.e., neglecting SO coupling) calculations. In this work we compare our energy band gaps directly with the experimental gaps.

All calculations were carried out using periodic boundary conditions (PBC), expanding Bloch functions in terms of

TABLE I. Calculated and experimental spin-orbit splittings (Δ_{SO}) and energy band gaps (E_g) for diamondlike Si and Ge. Experimental values were taken from Ref. 34.

System	Δ_{SO} (eV)		$E_{g,dir}$ (eV)		$E_{g,ind}$ (eV)	
	Calc.	Exp.	Calc.	Exp.	Calc.	Exp.
Si a_0=5.444 (Opt.)[a]	0.05	0.4	4.00	4.19	1.12	1.17
Si a_0=5.430 (Exp.)	0.05		4.10		1.12	
Ge a_0=5.701 (Opt.)[a]	0.28	0.30	0.47	0.90	0.63	0.74
Ge a_0=5.657 (Exp.)	0.28		0.76		0.73	

[a]Lattice parameter optimized with the HSE functional (taken from Ref. 4).

atomic Gaussian-type orbitals as implemented in the GAUSSIAN suite of programs.[22,23] Self-consistent Kohn-Sham calculations were performed on all systems. The short-range Hartree-Fock exchange interactions were calculated in real space using a specially adapted near-field exchange method[24] for screened interactions in PBC as implemented for the HSE functional.[25,26] Note that the screening parameter for the Hartree-Fock exchange used here and in all our previous papers for HSE was $\omega=0.15/\sqrt{2}$ Bohr^{-1} instead of the previously quoted 0.15 Bohr^{-1}.[12] Band gap dependence on the screening parameter is not crucial for ω values arround 0.15 Bohr^{-1} as will be reported elsewhere.[26] We have employed semilocal atomic-energy-consistent relativistic effective core potentials[27–29] (RECPs) for third (Cu, Zn, Ga, Ge, As, Se, Br) and fourth row elements (Ag, Cd, In, Sb, Te, I), and shape-consistent RECPs (Ref. 30) for second row elements (Mg, Al, Si, P, S, and Cl). For a general review on the choice of RECPs in DFT calculations the reader is referred to Ref. 31.

The corresponding matrix elements of the SO operator for a given RECP were evaluated following Refs. 32 and 33, adapted for PBC. The SO coupling was included in our calculations using the second variation approach.

For second row elements, we have employed the basis sets of Pacios and Christiansen[30] in fully uncontracted form and with all basis functions with exponents below 0.12 removed. In this way, we avoid the excessive computational

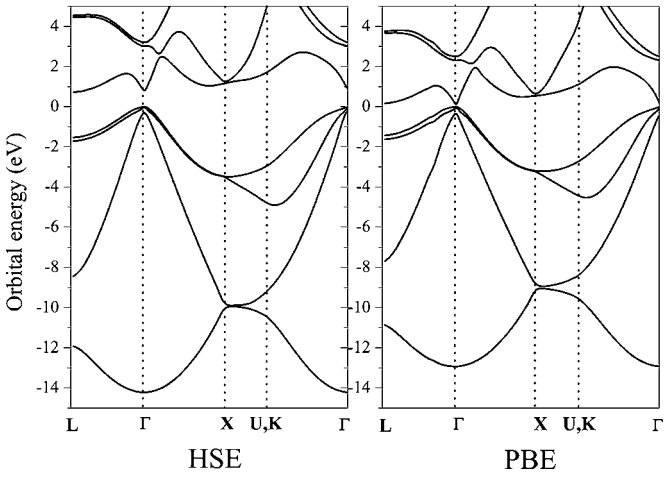

FIG. 1. Comparison of the band structure for Ge as calculated with the HSE functional (left panel) and the PBE functionals (right panel).

cost of including diffuse basis functions from basis sets tailored for atomic and molecular calculations which in our experience have negligible impact on the quality of the results for solids. For third and fourth row elements we have adopted the basis set given in Ref. 4, fully uncontracted. For Cu and Ag, we have utilized the double-zeta basis of Figgen *et al.*,[29] fully uncontracted with exponents below 0.12 removed also.

All systems considered in this paper are closed-shell. All calculations were carried out considering a diamond crystal structure for group IV elements and a zinc-blende crystal structure for all compounds, except AgCl and AgBr that were taken in the rocksalt structure. Reciprocal space integration was performed using a uniform k-space mesh of at least 24 points in each dimension. Band gaps and SO splittings were obtained as Kohn-Sham band energy differences. In all cases, band structure calculations were performed using the lattice parameters optimized with the HSE functional. With the exception of group IB-VII compounds, optimized lattice parameters were taken from Ref. 4. For group IB-VII compounds, we have optimized the lattice parameter with the HSE functional employing the basis set described above (op-

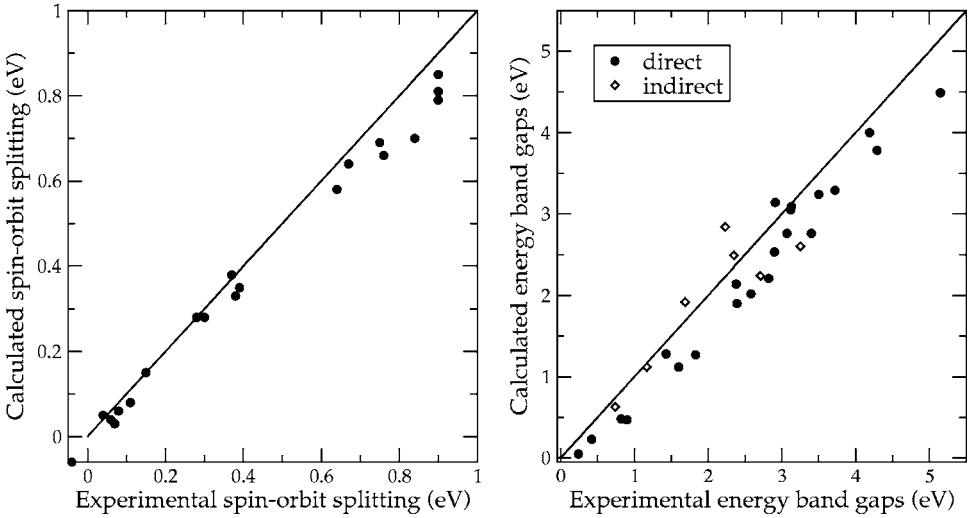

FIG. 2. Theoretical (HSE) vs experimental spin-orbit splitting (left panel) and energy band gaps (right panel).

TABLE II. Calculated and experimental spin-orbit splittings (Δ_{SO}) and energy band gaps (E_g) for group III-V, group II-VI, and group IB-VII compounds. For direct semiconductors, only $E_{g,dir}$ is reported. Unless otherwise indicated, experimental values were taken from Ref. 34.

	Δ_{SO} (eV)		$E_{g,dir}$ (eV)		$E_{g,ind}$ (eV)	
System	Calc.	Exp.	Calc.	Exp.	Calc.	Exp.
AlAs	0.28	0.28	3.09	3.13	2.84	2.23
AlSb	0.64	0.67	2.14	2.38	1.92	1.69
GaP	0.06	0.08	2.53	2.90	2.49	2.35
GaAs	0.31	0.35	1.08	1.52		
GaSb	0.66	0.76	0.48	0.82		
InP	0.08	0.11	1.28	1.43		
InAs	0.33	0.38	0.23	0.42		
InSb	0.69	0.81, 0.75[a]	0.05	0.24		
MgTe	0.79	0.90[b]	3.24	3.50		
ZnS	0.04	0.06	3.29	3.72		
ZnSe	0.38	0.42, 0.37[c]	2.21	2.82		
ZnTe	0.85	0.97, 0.90[b], 0.92[c]	1.90	2.39		
CdS	0.03	0.07	2.02	2.58		
CdSe	0.35	0.42, 0.39[d]	1.27	1.83		
CdTe	0.81	0.95, 0.90[e]	1.12	1.60		
γ-CuCl	−0.06	−0.04	2.76	3.40		
γ-CuBr	0.15	0.15	2.76	3.07		
γ-CuI	0.58	0.64	3.05	3.12		
AgCl	−0.10		4.49	5.15	2.60	3.25
AgBr	0.17		3.78	4.29	2.24	2.71
γ-AgI	0.70	0.84	3.14	2.91		
Mean error[f]		−0.05		−0.27		
Mean absolute error[f]		0.05		0.27		
Root mean square error[f]		0.06		0.35		

[a]Reference 37.
[b]Extrapolated from $Mg_xZn_{1-x}Te$ ($x \leq 0.407$) and corrected −0.50 eV due to the overestimation of the SO splitting in ZnTe, Ref. 38.
[c]Reference 39.
[d]Reference 40.
[e]Reference 41.
[f]Including Si and Ge.

timized lattice parameters are γ-CuCl, $a=5.471$ Å; γ-CuBr, $a=5.735$ Å; γ-CuI, $a=6.112$ Å; AgCl, $a=5.592$ Å; AgBr, $a=5.829$ Å; and γ-AgI, $a=6.632$ Å).

For the systems studied in this paper, SO splittings occur at the Γ point at the top of the valence band, $\Delta_{SO}=\epsilon(\Gamma_{8v})-\epsilon(\Gamma_{7v})$. Since the top of the valence band is dominated by the anion p-type orbitals, it is expected that Δ_{SO} is dominated by the atomiclike $\epsilon(p_{3/2})$-$\epsilon(p_{1/2})$ splitting of the anion, with some additional hybridization effects from the crystal environment.

In Table I we present HSE results for SO splittings and energy band gaps in carbon and silicon (group IV elements). For the sake of comparison, results at experimental lattice constants are also shown. For Si and Ge, direct band gaps ($E_{g,dir}$) are slightly underestimated with respect to the experiment, while indirect band gaps ($E_{g,ind}$) are in excellent agreement with experimental values. As it has been previously shown, standard functionals show a severe underestimation of band gaps.[4,6] Ge shows a stronger dependence of the band gaps on the lattice parameter than Si. SO splittings are almost insensitive to the choice of experimental or optimized lattice constant. Our HSE SO splittings are in close agreement with previous LDA calculations.[35,36] This is not surprising since SO splittings are mostly atomic in nature, and therefore largely determined by the SO part of the pseudopotential.

In Fig. 1, we compare the band structure for Ge as calculated with HSE and PBE at the experimental lattice constant. Even though at first sight both plots look similar, there are two qualitative differences. First, HSE predicts a finite energy gap at Γ of 0.76 eV, while PBE gives a small gap of 0.02 eV. The SO splitting of 0.28 eV at the topmost conduction band is observed in both cases at Γ. Second, HSE not only destabilizes conduction band energies compared to PBE, but also stabilizes the valence bands, and as a result,

HSE band widths are larger (14.1 eV) than those calculated with the PBE functional (12.8 eV).

In Table II, we present HSE SO splittings and energy band gaps for group III-V, II-VI, and IB-VII compounds. For some systems, reported experimental SO splittings are rather old, and for InSb, ZnSe, ZnTe, CdSe, and CdTe we found more than one different experimental value in the literature (the largest difference is 0.06 eV). Our calculations slightly underestimate SO splittings by 0.05 eV (mean error), with a mean absolute error of 0.05 eV. The largest discrepancy, 0.14 eV, corresponds to γ-AgI. This underestimation, however, cannot be directly attributed to the HSE functional, but rather to the RECPs employed and to the second-variational approach. We also note some discrepancies between the present RECP calculations.

Energy band gaps (taking SO splitting into account) calculated with HSE are underestimated on average by 0.27 eV (with a mean absolute deviation of 0.35 eV), in contrast to pure functionals, which yield an underestimation of more than 1 eV.[4] HSE errrors are similar to those obtained previously in Ref. 4 without including SO in the calculation and using a weighted average for the reference value. Here we explicitly show that the picture remains the same after including SO interaction and comparing with the actual experimental energy band gaps. This comparison as well as calculated versus experimental SO splittings is shown in Fig. 2.

In summary, we have shown that the HSE functional gives a very good estimate of energy band gaps and SO splittings in a set of 23 semiconductors. Considering these results and previous assessments of HSE for lattice constants and energy band gaps in semiconductors,[4,20] and structural and thermochemical properties of molecules,[13] the HSE functional provides a useful tool for practical applications in both molecular and extended systems.

This work was supported by the Department of Energy (Grant No. DE-FG02-01ER15232) and the Welch Foundation. In addition, R.L.M. is grateful for support from the DOE OBES Heavy Element Program and the LDRD Program at Los Alamos National Laboratory.

[1] J. Tao, J. P. Perdew, V. N. Staroverov, and G. E. Scuseria, Phys. Rev. Lett. **91**, 146401 (2003).
[2] V. N. Staroverov, G. E. Scuseria, J. Tao, and J. P. Perdew, Phys. Rev. B **69**, 075102 (2004).
[3] J. E. Peralta, J. Uddin, and G. E. Scuseria, J. Chem. Phys. **122**, 084108 (2005).
[4] J. Heyd, J. E. Peralta, G. E. Scuseria, and R. L. Martin, J. Chem. Phys. **123**, 174101 (2005).
[5] R. W. Godby, M. Schlüter, and L. J. Sham, Phys. Rev. Lett. **56**, 2415 (1986).
[6] J. Perdew, Int. J. Quantum Chem. **30**, 451 (1986).
[7] G. A. Baraff and M. Schlüter, Phys. Rev. B **30**, 3460 (1984).
[8] A. I. Liechtenstein, V. I. Anisimov, and J. Zaanen, Phys. Rev. B **52**, R5467 (1995).
[9] L. Kleinman and D. M. Bylander, Phys. Rev. Lett. **48**, 1425 (1982).
[10] W. G. Aulbur, L. Jonsson, and J. W. Wilkins, Solid State Phys. **54**, 1 (2000).
[11] A. D. Becke, J. Chem. Phys. **98**, 1372 (1993).
[12] J. Heyd, G. E. Scuseria, and M. Ernzerhof, J. Chem. Phys. **118**, 8207 (2003); **124**, 219906(E) (2006).
[13] J. Heyd and G. E. Scuseria, J. Chem. Phys. **120**, 7274 (2004).
[14] N. W. Ashcroft and N. D. Mermin, *Solid State Physics* (Saunders College Publishing, Orlando, Florida, 1976), p. 335.
[15] J. P. Perdew, K. Burke, and M. Ernzerhof, Phys. Rev. Lett. **77**, 3865 (1996).
[16] D. C. Langreth and J. P. Perdew, Solid State Commun. **17**, 1425 (1975).
[17] J. P. Perdew, M. Ernzerhof, and K. Burke, J. Chem. Phys. **105**, 9982 (1996).
[18] M. Ernzerhof and G. E. Scuseria, J. Chem. Phys. **110**, 5029 (1999).
[19] C. Adamo and V. Barone, J. Chem. Phys. **110**, 6158 (1999).
[20] J. Heyd and G. E. Scuseria, J. Chem. Phys. **121**, 1187 (2004).
[21] J. Paier, M. Marsman, K. Hummer, G. Kresse, I. C. Gerber, and J. G. Ángyán, J. Chem. Phys. **124**, 154709 (2006).
[22] K. N. Kudin and G. E. Scuseria, Phys. Rev. B **61**, 16440 (2000).
[23] M. J. Frisch, G. W. Trucks, H. B. Schlegel, G. E. Scuseria, M. A. Robb, J. R. Cheeseman, J. A. Montgomery, Jr., T. Vreven, K. N. Kudin *et al.*, *Gaussian Development Version, Revision C.01* (Gaussian, Inc., Pittsburgh, 2004).
[24] J. C. Burant, G. E. Scuseria, and M. J. Frisch, J. Chem. Phys. **105**, 8969 (1996).
[25] A. Izmaylov, G. E. Scuseria, and M. J. Frisch (unpublished).
[26] A. Krukau, A. Izmaylov, O. Vydrov, and G. E. Scuseria (unpublished).
[27] B. Metz, H. Stoll, and M. Dolg, J. Chem. Phys. **113**, 2563 (2000).
[28] K. A. Peterson, D. Figgen, E. Goll, H. Stoll, and M. Dolg, J. Chem. Phys. **119**, 11113 (2003).
[29] D. Figgen, G. Rauhut, M. Dolg, and H. Stoll, Chem. Phys. **311**, 227 (2005).
[30] L. F. Pacios and P. A. Christiansen, J. Chem. Phys. **82**, 2664 (1985).
[31] P. Pyykkö and H. Stoll, *in R.S.C. Specialist Periodical Reports: Chemical Modelling, Applications and Theory* (The Royal Society of Chemistry, London, 2000), Vol. 1, Chap. 5, p. 239.
[32] R. M. Pitzer and N. W. Winter, J. Phys. Chem. **92**, 3061 (1988).
[33] R. M. Pitzer and N. W. Winter, Int. J. Quantum Chem. **40**, 773 (1991).
[34] O. Madelung, *Semiconductors: Data Handbook*, 3rd ed. (Springer, New York, 2004).
[35] M. S. Hybertsen and S. G. Louie, Phys. Rev. B **34**, 2920 (1986).
[36] P. Carrier and S.-H. Wei, Phys. Rev. B **70**, 035212 (2004).
[37] C. Jung and P. R. Bressler, J. Electron Spectrosc. Relat. Phenom. **78**, 503 (1996).
[38] B. Montegu, A. Laugier, and D. Barbier, Phys. Rev. B **19**, 1920 (1979).
[39] A. Ebina, Y. Sato, and T. Takahashi, Phys. Rev. Lett. **32**, 1366 (1974).
[40] Y. D. Kim, M. V. Klein, S. F. Ren, Y. C. Chang, H. Luo, N. Samarth, and J. K. Furdyna, Phys. Rev. B **49**, 7262 (1994).
[41] D. T. F. Marple and H. Ehrenreich, Phys. Rev. Lett. **8**, 87 (1962).